

Concentration distributions of dissolved Sb(III) and Sb(V) species in size-classified inhalable airborne particulate matter†‡

Akihiro Iijima,^{*a} Keiichi Sato,^b Tomohiro Ikeda,^c Hikaru Sato,^c Kuniyoshi Kozawa^a and Naoki Furuta^c

Received 2nd October 2009, Accepted 3rd December 2009

First published as an Advance Article on the web 22nd December 2009

DOI: 10.1039/b920597g

In order to obtain more accurate assessments of global contamination by potentially toxic antimony (Sb) and the toxicological effects of Sb on ecosystems, speciation analysis of inorganic Sb species in size-classified airborne particulate matter (APM) was performed. Thirteen fractions of size-classified APM (with aerodynamic diameters: $D_p < 0.06$, 0.06–0.12, 0.12–0.20, 0.20–0.30, 0.30–0.50, 0.50–0.70, 0.70–1.2, 1.2–2.1, 2.1–3.6, 3.6–5.2, 5.2–7.9, 7.9–11, and $> 11 \mu\text{m}$) were collected on a filter by using a multistage cascade impactor sampler. Speciation analysis of inorganic Sb(III) and Sb(V) was performed by using HPLC-ICP-MS. Portions of sample-loaded filters were sonicated with 30 mmol l⁻¹ citric acid under purified N₂ in order to avoid the oxidation of Sb(III) to Sb(V) during the extraction process. Sb(III) and Sb(V) were separated on a PRP-X100 anion exchange column using a mixture of 10 mmol l⁻¹ EDTA and 1 mmol l⁻¹ phthalic acid (pH 4.5) as a mobile phase, and they were subsequently detected by ICP-MS. The size distributions of the total Sb concentration exhibit a bimodal profile in which peaks corresponded to fine (0.50–0.70 μm) and coarse (3.6–5.2 μm) fractions. The speciation analysis demonstrated for the first time that Sb(III), which is the more toxic form, is dominated by coarse fractions whereas Sb(V) is distributed in both the fine and coarse fractions. The presented high-resolution size distributions of inorganic Sb species will provide helpful information in discussing both health risks by inhalation exposure to Sb and the extent of the effects of emission sources by atmospheric circulation.

1. Introduction

In recent years, applications of antimony (Sb) compounds to industrial and commercial materials have increased, *e.g.*, Sb compounds are being widely used as flame retardants for plastic products or chemical fabrics, as hardening agents in lead alloys for batteries, as polycondensation catalysts in the production of polyethylene terephthalate (PET) containers, and as lubricants for friction materials.¹ Consequently, many literatures exist on the extraordinary enrichment of Sb in environmental samples such as airborne particulate matter (APM),^{2–4} soil,⁵ sediment,⁶ peat bog,^{7,8} and polar ice.⁹ As a result of the observations in these studies, Sb contamination has been recognized to be a global concern; further, APM has become well known as a carrier of the

contaminant in the global atmospheric circulation. The possibility of exposure to potentially toxic Sb compounds has gradually increased, and therefore, awareness of the adverse effects of Sb on the ecosystem and environment has also arisen.¹

Speciation analysis is extremely useful in gaining an understanding about the effects of an element on ecosystems because elemental behaviors, such as toxicity, bioavailability, and metabolic characteristics, are strongly dependent on its chemical form. In the case of the toxicity of Sb, the determination of redox species is particularly important. Inorganic Sb compounds generally exist as trivalent (Sb(III)) or pentavalent (Sb(V)) oxidation states, and Sb(III) compounds are generally more toxic than Sb(V) forms.¹⁰ Numerous methods for the Sb speciation analysis have been developed in previous years.¹¹ Among them, a hydride generation (HG) technique has been widely applied for the selective determination of inorganic Sb(III) and Sb(V). However, in this method, Sb(V) is not measured directly, but it is calculated by subtracting the concentration of Sb(III) from the total Sb concentration. A hyphenated technique, such as HPLC-ICP-MS, is more preferable because the high separation power provided by HPLC and the high sensitivity offered by ICP-MS make it feasible to determine Sb(III) and Sb(V), as well as organoantimony species, simultaneously at ultratrace levels.¹² Further, we must focus on sample preparation for the Sb speciation analysis because Sb(III) might oxidize to Sb(V) during the sample storage, extraction, and determination. In our previous study, it was demonstrated that Sb(III) spiked into a moat water sample was oxidized to Sb(V) within 30 min due to the presence of oxidizing substances in the bulk sample.¹² Similar phenomena

^aGunma Prefectural Institute of Public Health and Environmental Sciences, 378 Kamioki, Maebashi, Gunma, 371-0052, Japan. E-mail: iijima-akihiro@pref.gunma.jp; Fax: +81-27-234-8438; Tel: +81-27-232-4881

^bData Management Department, Acid Deposition and Oxidant Research Center, 1182 Sowa, Nishi-ku, Niigata, 950-2144, Japan

^cFaculty of Science and Engineering, Department of Applied Chemistry, Chuo University, 1-13-27 Kasuga, Bunkyo-ku, Tokyo, 112-8551, Japan

† This article is part of a themed issue devoted to highlighting the work of outstanding young analytical scientists (YAS) working in the area of analytical atomic spectrometry. This 3rd YAS issue has been guest edited by Professor Spiros Pergantis.

‡ Electronic supplementary information (ESI) available: Table S1: Analytical results of National Institute of Standard and Technology (NIST) SRM 1648. Table S2: Elemental concentrations in size-classified airborne particulate matter (APM). See DOI: 10.1039/b920597g

have been observed by many researchers.^{13,14} It has been reported that a Sb(III) solution could be stabilized for 12 months by storage in 50 mmol l⁻¹ citric acid solution.¹⁵ Hence, in a previous study, we examined the complexation effect of Sb compounds with citric acid and developed its application to the speciation of Sb(III) and Sb(V) in environmental samples using HPLC-ICP-MS.¹² Our novel analytical method enabled the prevention of the oxidation of Sb(III) to Sb(V) by forming complex ions of Sb(III)-citrate and Sb(V)-citrate, and the existence of Sb(III), the more toxic form, in APM samples was demonstrated for the first time. Many other researches applying this method have been performed on volcanic ash,¹⁶ coal fly ash,¹⁷ and soil samples.^{5,18}

To assess the health risks of Sb compounds, the route of exposure must be considered along with the determination of chemical species.¹⁹ In particular, two routes—*inhalation* and *ingestion*—are supposed to be the dominant exposure routes of Sb from the environment. The dose of Sb *via* ingestion has been estimated to be greater than that *via* inhalation.²⁰ However, the inhalation exposure to Sb should be more emphasized from the toxicological viewpoints. Many animal experiments examining the effects of the inhalation exposure to particulate Sb(III) species have revealed potential risks of the occurrence of adverse effects on respiratory and/or cardiovascular systems.^{21–23} Although the currently available data on the carcinogenicity of Sb compounds can be regarded as inconclusive, epidemiological studies on individuals who were occupationally exposed to Sb compounds have demonstrated greater risks of death by various types of cancers, cardiovascular diseases, and cerebrovascular diseases than individuals from the control groups.^{24,25} Therefore, the inhalation exposure to Sb compounds, which was mainly caused by the inhalation of APM, can be considered to be one of the most important routes enhancing the health risks of this element. Since the deposition efficiency of APM onto respiratory tracts strongly depends on the particle size of the APM, more information regarding both the particle size and oxidation states of Sb in APM is required for a better risk assessment.

We recently demonstrated high-resolution size distributions of multielement concentrations in size-classified APM that were collected by using a multistage cascade impactor sampler.²⁶ This sampler enables the collection of inhalable APM samples along with their classification into 13 different size fractions. Sb concentration in size-classified APM showed a characteristic bimodal profile in which peaks corresponding to fine (0.50–0.70 μm) and coarse (3.6–5.2 μm) fractions were obtained. By considering the similarities in particle size and elemental composition between ambient APM and several potential source samples, waste fly ash and automotive brake abrasion dust were identified as the predominant sources of Sb in the fine and coarse APM, respectively.²⁶ The combination of the established speciation analysis of Sb(III) and Sb(V)¹² and the demonstrated high-size resolution sampling of APM²⁶ was expected to enable the determination of Sb species in size-classified APM samples. Hence, in the present study, 13 fractions of size-classified APM samples were collected at two different locations, and multielement analysis and speciation analysis of Sb were performed. The concentration distributions of total Sb, Sb(III), and Sb(V) in size-classified APM were determined. In addition, the speciation analysis of Sb was also applied to the samples collected from the abovementioned two predominant Sb sources. Furthermore, the

effects of Sb species on the ecosystem and environment were discussed.

2. Experimental

2.1. Chemicals and reagents

All the chemicals and reagents used in the present study were of analytical grade. Milli-Q purified water (resistivity: 18.3 MΩ cm) (Milli-Q Gradient, Nihon Millipore K. K., Tokyo, Japan) was used throughout all of the analyses. HF (50%), HNO₃ (60%), H₂O₂ (30%), NH₄OH (30%), ethylenediaminetetraacetic acid (EDTA), phthalic acid, and citric acid were obtained from Kanto Chemical Co., Inc. (Tokyo, Japan). A multielement standard solution containing Be, Na, Mg, Al, K, Ca, V, Cr, Mn, Fe, Co, Ni, Cu, Zn, As, Se, Mo, Ag, Cd, Sb, Ba, Tl, Pb, Th, and U (10 μg ml⁻¹ each) (AccuTrace™ Reference Standard ICP-MS Quality Control Sample 2) was purchased from AccuStandard, Inc. (New Haven, CT, USA). Standard solutions of In and Bi (1000 μg ml⁻¹ each) for internal correction were obtained from Kanto Chemical Co., Inc. Working multielement standard solutions for calibration were prepared by diluting with 0.1 mol l⁻¹ HNO₃. A stock solution of Sb(III) was prepared from a commercially available 1000 μg ml⁻¹ standard solution (SbCl₃ in diluted HCl, Kanto Chemical Co., Inc.). A stock solution of Sb(V) was prepared from potassium hexahydroxoantimonate(V) (Kanto Chemical Co., Inc.). Working standard solutions of Sb(III) and Sb(V) for speciation were prepared by diluting the stock solutions with 30 mmol l⁻¹ citric acid.

2.2. Instrumentation

Sample digestion was performed by using a microwave oven (Multiwave 3000, Anton Paar GmbH, Graz, Austria). The ICP-MS instrument used for the multielement analysis was Agilent 7500cx (Agilent Technologies, Inc., Tokyo, Japan). To avoid the spectral interferences caused by Ar- or matrix-derived polyatomic ions, the multielement analysis was conducted under collision, reaction, or non-gas modes appropriately for each element.

A chromatographic system consisting of an HPLC pump (JASCO PU-1580I, JASCO Corporation, Tokyo, Japan), a syringe-loading injector with a 100 μl loop, and an inert anion exchange column (PRP-X100, Hamilton Company, Reno, NV, USA) was used. The ICP-MS instrument used for the speciation analysis of Sb was HP 4500 (HP 4500, Agilent Technologies, Inc.). The chromatographic system was interfaced with an ICP-MS instrument using a PEEK (polyether ether ketone) capillary tube to connect the column outlet to the inlet of the nebulizer. The operating conditions for the ICP-MS and HPLC-ICP-MS are summarized in Table 1.

2.3. Collection of size-classified APM

Size-classified samples of APM were collected from a roadside site (Tatebayashi) and a residential site (Maebashi). The descriptions of the sampling sites and procedures were given in detail in our previous study.²⁶ In brief, Tatebayashi is located at the intersection of heavy-traffic national highways. Maebashi is located in a residential area of a small city in a northwestern

Table 1 Operating conditions for ICP-MS and HPLC-ICP-MS instruments

<i>ICP-MS</i>	
Instrument	Agilent 7500cx
Plasma power	1600W
Plasma Ar flow	15.0 l min ⁻¹
Auxiliary Ar flow	1.0 l min ⁻¹
Nebulizer Ar flow	1.0 l min ⁻¹
Make-up Ar flow	0.2 l min ⁻¹
Sampling depth	8.5 mm
Collision gas (He) flow	4.5 ml min ⁻¹
Reaction gas (H ₂) flow	5.0 ml min ⁻¹
Collision/reaction cell	Octopole reaction cell
Measurement mode	Peak hopping analysis
Integration time	300 ms
Replicates	3
Internal standard	¹¹⁵ In and ²⁰⁹ Bi
<i>HPLC-ICP-MS</i>	
<i>HPLC</i>	
Instrument	JASCO PU-15801
Column	Hamilton PRP-X100 (250 × 4.6 mm id)
Column temperature	Ambient
Mobile phase	10 mmol l ⁻¹ EDTA + 1 mmol ⁻¹ phthalic acid at pH 4.5
Flow rate	0.6 ml min ⁻¹
Injection Volume	100 μl
<i>ICP-MS</i>	
Instrument	HP 4500
Plasma power	1300 W
Plasma Ar flow	15.0 l min ⁻¹
Auxiliary Ar flow	1.0 l min ⁻¹
Nebulizer Ar flow	1.0 l min ⁻¹
Sampling depth	5.0 mm
Measurement mode	Time resolved analysis
Integration time	100 ms
Total analysis time	800 s

suburban area situated 100 km away from the center of Tokyo and 50 km west away from the roadside site. The sampling period were from Oct. 29, 2008 to Nov. 5, 2008 and Nov. 5, 2008 to Nov. 13, 2008 for the roadside and residential sites, respectively. Thirteen fractions of size-classified APM (with aerodynamic diameters: $D_p < 0.06$, 0.06–0.12, 0.12–0.20, 0.20–0.30, 0.30–0.50, 0.50–0.70, 0.70–1.2, 1.2–2.1, 2.1–3.6, 3.6–5.2, 5.2–7.9, 7.9–11, and > 11 μm) were collected on Polyflon® filters (PF 020 for the finest fraction, PF 060 for the other fractions; Toyo Roshi Kaisha, Ltd., Tokyo, Japan) by using an Andersen-type low-pressure-impactor (LPI) air sampler (LP-20; Tokyo Dylec Co., Japan).

2.4. Collection of waste fly ash and brake abrasion dust samples

The procedures of sample collection of the waste fly ash and brake abrasion dust used have been described in our previous studies.^{26–28} In brief, powder-formed waste fly ash samples were collected from electric precipitators in different incinerators and stored in glass vials. Abrasion dust particles from an automotive brake were generated by using a brake dynamometer. Three types of commercially available brake pads were used. Dust particles were discharged into an enclosed chamber and subsequently collected on a quartz fiber filter (2500 QAT-UP; 180 × 230 mm, Pall Corporation, Port Washington, NY, USA) by

using a high-volume air sampler (Model 120V; Kimoto Electric Co., Ltd., Osaka, Japan).

2.5. Multielement analysis of size-classified APM

One quarter of the sample-loaded filters were digested in a mixture of 2 ml of HF, 5 ml of HNO₃, and 1 ml of H₂O₂ in a microwave digestion system at 700 W for 10 min and 900 W for a further 30 min. HF was evaporated by heating the sample solution at 200 °C on a hot plate, and 0.1 mol l⁻¹ HNO₃ was subsequently added to obtain 50 ml of the sample. The concentrations of Sb and other trace elements (Be, V, Cr, Mn, Co, Ni, Cu, Zn, As, Se, Mo, Ag, Cd, Ba, Tl, Pb, Th, and U) in the final solutions were determined by ICP-MS. All the analytical procedures were validated by using the standard reference material (SRM) 1648, urban particulate matter that was prepared by the US National Institute of Standard and Technology (NIST). The analytical results are listed in Supplementary Table S1.† They were in good agreement with the certified or reference values.

2.6. Speciation analysis of Sb(III) and Sb(V) in size-classified APM and potential source samples

Another quarter of the sample-loaded filters of size-classified APM were introduced into polycarbonate containers (capacity: 100 ml), and then, 20 ml of 30 mmol l⁻¹ citric acid was added. The containers were sonicated under purified N₂ for 30 min at room temperature in an ultrasonic bath. The resulting solutions were filtered by using a cellulose nitrate filter (pore size: 0.45 μm, Nihon Millipore K. K.).

Approximately 50 mg of fly ash samples were introduced into polycarbonate containers and treated using procedures identical to those described above. The filtrates were further diluted 20-fold using 30 mmol l⁻¹ citric acid for the speciation analysis. Portions of the sample-loaded filters (47 mmφ) of brake abrasion dust were placed in polycarbonate containers and treated using procedures identical to those described above. The filtrates were further diluted 100-fold using 30 mmol l⁻¹ citric acid for the speciation analysis.

The total dissolved Sb concentrations in the filtrate extracts were analyzed by ICP-MS prior to the speciation analysis. Subsequently, speciation analysis of Sb(III) and Sb(V) was performed by using HPLC-ICP-MS. A mixture of 10 mmol l⁻¹ EDTA and 1 mmol l⁻¹ phthalic acid was used as a mobile phase. The pH of the mobile phase was adjusted to 4.5 by the dropwise addition of 30% NH₄OH and 1 mol l⁻¹ HNO₃. Owing to a series of optimization of HPLC-ICP-MS in our previous work,¹² good separation between Sb(III) and Sb(V) could be achieved.

3. Results and discussion

3.1. Overview of the concentration distributions of Sb and other relevant elements in size-classified APM

The mass concentration distributions of Sb and other relevant elements, Cu, Ba, Cd, and Pb, in size-classified APM at the roadside and residential sites are shown in Fig. 1. The relationship among these five elements has already been discussed in detail in our previous study,²⁶ which was aimed at the

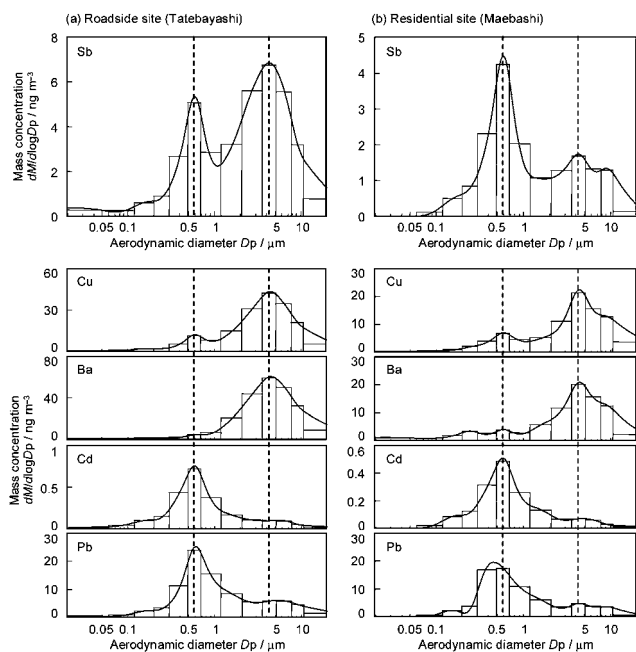


Fig. 1 Concentration distributions of Sb, Cu, Ba, Cd, and Pb in size-classified airborne particulate matter (APM) collected at (a) the roadside site and (b) the residential site. The solid curve indicates a smoothed distribution and the broken lines represent the diameters of the peaks of the fine and coarse fractions as seen in the Sb concentration distributions.

identification of the predominant sources of Sb in APM. In the present study, other sets of size-classified APM samples were collected again at the same sites for the speciation analysis of Sb. At first, we tried to confirm the representativeness of the newly collected samples prior to the discussion on Sb species.

As shown in Fig. 1, the size distributions of Sb concentrations at both the sites exhibit a bimodal profile having two peaks, one corresponding to fine (0.50–0.70 μm) and other to coarse (3.6–5.2 μm) fractions. This bimodal profile of Sb is unique among those of the other elements measured. The coarser fraction peak was considerably higher at the roadside site than at the residential site distribution. The distribution of Sb in coarse fractions is similar to those observed in Cu and Ba, whereas the distribution of Sb in fine fractions is similar to those in Cd and Pb. These features are also similar to those observed in the previous study.²⁶

The concentrations of all the elements determined in 13 size fractions were merged into 3 size ranges ($D_p < 2.1$, 2.1–11, and $> 11 \mu\text{m}$); they are listed in Supplementary Table S2.† The total Sb concentrations at the roadside and residential sites were 8.1 ng m^{-3} and 3.3 ng m^{-3} , respectively (it must be noted that the y axis in Fig. 1 has a scale of $dM/d\log D_p$, where M is mass concentration). These data were relatively higher than those observed in the previous study (3.7 ng m^{-3} at the roadside site and 2.7 ng m^{-3} at the residential site).²⁶ Similarly, the concentrations of most of the other elements observed in the present study were relatively higher than those in the previous data. Sample collection was carried out during the dry autumn season (October to November) in the present study, whereas it was conducted during the wet summer season (August to September) in the previous study. The increase in the elemental concentrations might be due to the differences in the meteorological conditions. Typical

elemental concentrations at the residential site have been extensively investigated in a long-term monitoring study conducted from 2003 to 2006;⁴ the average Sb concentration in fine ($D_p < 2.1 \mu\text{m}$) APM was found to be 2.17 ng m^{-3} . The average Sb concentration in fine ($D_p < 2.1 \mu\text{m}$) APM in the present study (2.2 ng m^{-3} , see Supplementary Table S2‡) is very similar to the typical concentration. Consequently, the data obtained in the present study can be considered to represent the typical conditions.

3.2. Concentration distributions of dissolved Sb(III) and Sb(V) in size-classified APM

A representative chromatogram obtained using a standard solution containing Sb(III)-citrate and Sb(V)-citrate (5 ng Sb ml^{-1} each) in the present study is shown in Fig. 2. Hansen and Pergantis²⁹ have reported that Sb(III)-citrate would be converted to Sb(III)-EDTA on the column under the relevant chromatographic condition (EDTA in the mobile phase). Therefore, we simply described the first and second peaks seen in Fig. 2 as Sb(III) and Sb(V), respectively. Low detection limits of 0.05 and 0.08 ng ml^{-1} were obtained in the case of Sb(III) and Sb(V), respectively. The precisions, which were evaluated by using the relative standard deviation (%RSD) with a 1 ng ml^{-1} standard solution, were 2.0% and 4.7% ($n = 3$) for Sb(III) and Sb(V), respectively.

Fig. 3 shows the obtained chromatograms for the respective size fractions of APM collected at the roadside site. Since no significant Sb signals were observed from two fine fractions ($D_p < 0.06$ and 0.06–0.12 μm), these data were excluded from further discussions. As shown in Fig. 3, two dominant peaks were clearly separated and identified as Sb(III) and Sb(V), respectively, by an agreement with the retention times of the respective standard solutions. The compositions of Sb(III) and Sb(V) are fairly different for different particle sizes. Sb(III) dominates in the coarse fractions ($D_p > 1.2 \mu\text{m}$) whereas Sb(V) is distributed in both the fine and coarse fractions.

We should note here that slight oxidation of Sb(III) to Sb(V) occurred. Our preliminary experiment has revealed that approximately 5% of Sb(III) was oxidized to Sb(V) during the sonication despite the use of citric acid. Although the extraction time and efficiency were considerably improved by using an ultrasonic bath, excessive oxidizing substances might also be generated. Then the peak areas of Sb(III) and Sb(V) were corrected and the concentrations of respective species were

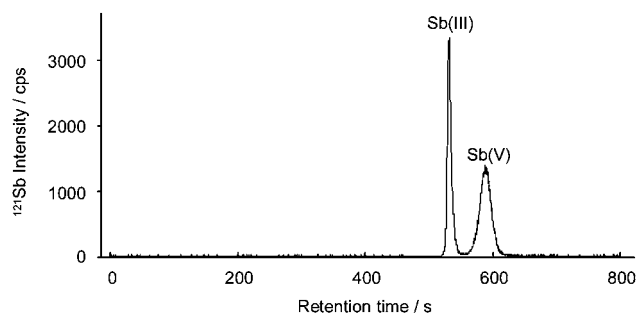


Fig. 2 Chromatographic separation of Sb(III) and Sb(V) (5 ng Sb ml^{-1} each).

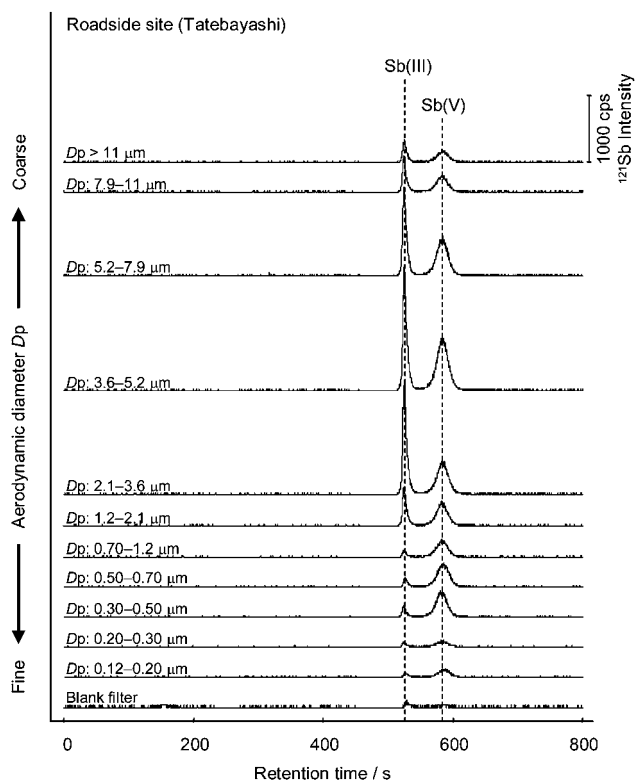


Fig. 3 Chromatograms of size-classified airborne particulate matter (APM) collected at the roadside site. Citric acid was used as an extractant, and the sample-loaded and blank filters were sonicated under purified N_2 .

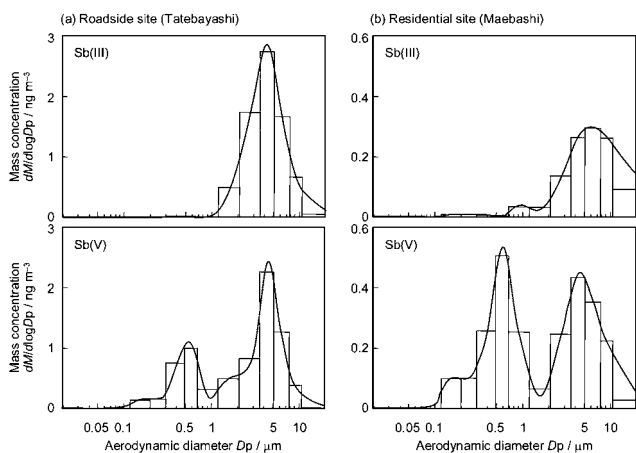


Fig. 4 Distributions of Sb(III) and Sb(V) concentration in size-classified airborne particulate matter (APM) collected at (a) the roadside site and (b) the residential site. The solid curve indicates a smoothed distribution.

calculated. Fig. 4 shows the concentration distributions of Sb(III) and Sb(V) in size-classified APM at the roadside and residential sites. Characteristic particle size-dependent distributions of Sb(III) and Sb(V) were observed in both the results obtained at the roadside and residential sites. Although we have already successfully determined Sb(III) and Sb(V) contained in bulk APM sample in our previous study,¹² their high-resolution

size distributions are demonstrated for the first time in the present study.

Table 2 summarizes the concentrations of digested Sb, extracted Sb, and dissolved inorganic Sb species in the two peak fractions of the size-classified APM. In the case of the fine peak fractions, 26–28% of the total Sb was extracted with citric acid. As mentioned above, Sb(V) was the dominant species in the fine fractions in both the sites. However, the determined Sb species remained at 47–72% of the extracted Sb concentrations. In particular, a relatively low yield (47%) was obtained at the residential site, which indicates that non-negligible amounts of unknown species exist in the fine fractions. Zheng *et al.*³⁰ detected trimethylantimony (TMSb) and other several unknown Sb species from the water extract of bulk APM sample collected at Tokyo, Japan. Methylated Sb species were detected from various environmental samples such as soil³¹ and plant,³² which suggests that organoantimony species participate in the biogeochemical cycles of Sb in the environment. In this study, no signals implying the existence of these organoantimony species could be detected. Chromatographic condition applied in the present study was not suitable to elute these species.³² On the other hand, in the coarse peaks, 44–88% of the total Sb was extracted with citric acid. Relatively high extraction efficiency (88%) was observed at the roadside site, and Sb(III) was more abundant than Sb(V). The yields of the determined Sb species accounted for 82–93% of the extracted Sb concentrations, indicating that both inorganic Sb(III) and Sb(V) were dominant in the extracted Sb from coarse APM.

The demonstrated characteristic size distributions of Sb(III) and Sb(V) suggest that further discussions on the effects of Sb on the ecosystem and environment are required. In terms of the health risks on humans, the effects of inhalation exposure to airborne Sb can then be assessed more properly. A reliable lung deposition model, the human respiratory tract model for radiation protection has been developed by the International Commission on Radiological Protection³³ for the purpose of safety assessment of radiation exposure. Micron-sized particles are selectively deposited onto the upper parts of respiratory tracts. In the case of coarse particles with $D_p = 4 \mu\text{m}$, approximately 80% of the total particles are deposited onto the nasal cavity, pharynx, and larynx. On the other hand, submicron-sized particles show a relatively low total deposition rate (30–40%). Nevertheless, submicron-sized particles have a greater tendency to deposit onto the lower respiratory tracts including bronchioles and alveolar ducts than micron-sized particles. Nanosized particles are selectively deposited onto the lowest part of respiratory tracts. According to this model, fine particles are considered to be more toxic than coarse particles. However, when we focus on the inhalation exposure to Sb, we must also pay attention to the upper part of respiratory tracts because of the existence of more toxic Sb(III) compounds.

With respect to environmental effects, the results presented enable a better understanding on the atmospheric circulation of Sb from local to global levels. In general, fine particles have a long residence time, causing a global contamination as a result of atmospheric circulation. The historical archives of Sb contamination recorded in background peat cores^{7,8} and in polar ice cores⁹ are most likely to be affected by the deposition of fine APM primarily containing Sb(V) carried by global atmospheric

Table 2 Analytical results of Sb in the peak fractions of size-classified airborne particulate matter (APM)

Peak fraction	Site	Total Sb ^a /ng m ⁻³		Efficiency ^b /%	Inorganic Sb species ^a /ng m ⁻³		Yield ^c /%
		Digested	Extracted		Sb(III)	Sb(V)	
Fine (0.5–0.7 μm)	Roadside	0.74(5.1)	0.21(1.4)	28	0.0008(0.005)	0.15(0.99)	72
	Residential	0.62(4.2)	0.16(1.1)	26	0.0004(0.003)	0.074(0.51)	47
Coarse (3.6–5.2 μm)	Roadside	1.1(6.8)	0.97(6.1)	88	0.44(2.7)	0.36(2.3)	82
	Residential	0.27(1.7)	0.12(0.74)	44	0.042(0.26)	0.069(0.43)	93

^a Values with a scale of $dM/d\log Dp$ (ng m⁻³) are listed following the measured mass concentrations in parentheses. ^b Values were calculated as the concentration ratios of [extracted Sb] to [digested Sb]. ^c Values were calculated as the concentration ratios of [Sb(III) + Sb(V)] to [extracted Sb].

circulation. On the contrary, the effects of coarse particles may be dominant in the vicinity of the emission sources. Sb contamination found in soils^{5,18} in the vicinity of road traffic can be attributed to the deposition of coarse APM containing both Sb(III) and Sb(V).

3.3. Determination of Sb(III) and Sb(V) in the predominant sources of Sb in APM

According to the substance flow analysis of Sb in Japan, approximately 13,400 tons of Sb was supplied for domestic use in 2003.³⁴ Antimony trioxide (Sb₂O₃) accounts for a large share (12,600 tons) of the supply; it is mainly used as a flame retardant for various plastic products. Antimony trisulfide (Sb₂S₃) accounts for a small share (75 tons) of the supply, and it is mainly used as a solid lubricant for automotive brake pads. Despite the considerable domestic demand for Sb(III) compounds, it is noteworthy that significant amounts of Sb(V) were obtained from size-classified APM samples. In Japan, waste fly ash and automotive brake abrasion dust are the predominant sources of Sb in fine and coarse APM, respectively, as demonstrated in our previous study.²⁶ Hence, speciation analysis of Sb was also performed for the samples collected from the abovementioned two predominant sources. Table 3 summarizes the concentrations of digested Sb, extracted Sb, and dissolved inorganic Sb species in the source samples. Due to the limited amount of samples, all the experiments were performed once for each sample, and three different types of the samples were investigated for the respective sources.

In the case of the waste fly ash samples, 11–56% of the total Sb was extracted with citric acid. Difference in the extraction efficiencies is attributed to the wide diversity of incinerated wastes in different incinerators. Sb(V) is the dominant species in all the samples; this result is similar to that observed in the case of the fine fractions of APM samples. Household wastes are generally contaminated with various types of Sb-containing plastic products. Chandler *et al.*³⁵ reported that high-volatile SbCl₃ can be formed in the incinerator and transformed to Sb₂O₃ by hydrolysis; however, the present data does not support this assertion. Takahashi *et al.*³⁶ demonstrated that the originally present Sb(III) compounds can be partially oxidized to Sb(V) during the manufacturing processes of the production of plastic materials. Moreover, the remaining Sb(III) may be oxidized to Sb(V) under the high-temperature (more than 800 °C) incineration process. The yields of the determined Sb species accounted for 96–103% of the extracted Sb concentrations, indicating that inorganic Sb(V) dominates the extracted Sb in waste fly ash samples. As mentioned above, the yields of the determined Sb species in the fine peaks of APM were relatively low, implying the existence of several unknown Sb species. Therefore, transformation from an inorganic Sb(V) species to an unidentified species during atmospheric circulation is another interest of the fates of Sb in the environment.

In the case of the brake abrasion dust samples, 48–65% of the total Sb was extracted with citric acid. Sb(III) was more abundant than Sb(V); this result is similar to that observed in the coarse fractions of APM samples. As mentioned above, Sb₂S₃ is used in automotive brake pads. Uexküll *et al.*³⁷ examined the

Table 3 Analytical results of Sb in the samples collected from the predominant sources of airborne Sb

Predominant source	Sample ID	Total Sb/μg g ⁻¹		Efficiency ^a /%	Inorganic Sb species/μg g ⁻¹		Yield ^b /%
		Digested	Extracted		Sb(III)	Sb(V)	
Waste fly ash ^c	wfa01	370	40	11	1.6	39	101
	wfa02	960	300	31	7.9	280	96
	wfa03	630	350	56	12	350	103
Brake abrasion dust ^d	bad01	7800	4700	60	3000	1600	98
	bad02	17000	11000	65	6600	3300	90
	bad03	19000	9100	48	4900	4500	103

^a Values were calculated as the concentration ratios of [extracted Sb] to [digested Sb]. ^b Values were calculated as the concentration ratios of [Sb(III) + Sb(V)] to [extracted Sb]. ^c Powder-formed waste fly ash samples were collected from electric precipitators in different incinerators in our previous study.²⁶ ^d Abrasion dust particles were generated by using a brake dynamometer under typical urban district driving conditions (initial driving speed: 50 km h⁻¹; deceleration: 2 m s⁻²). Three types of commercially available brake pads were used. Dust samples (referred to as bad01, bad02, and bad03) are the same samples (labeled run nos. 5, 11, 14, respectively) collected in our previous study.²⁸

extraction efficiencies of several Sb(III) compounds by using 10% tartaric acid as an extractant. The extraction efficiency of Sb_2S_3 was 10%; however, it increased to 34% when the sample powder was heated for 30 min at 400 °C prior to the extraction. Although the mechanisms of the changes in the physicochemical properties of Sb_2S_3 have not been addressed, this is a piece of evidence indicating that friction heat changes the chemical form of Sb to a more soluble species. Uexküll *et al.*³⁷ also referred to the formation of intermediate products such as Sb_2O_3 , $\text{Sb}_2(\text{SO}_4)_3$, and Sb_2OS_2 by friction heat of braking process. The present results suggest that significant changes in the oxidation states from Sb(III) to Sb(V) have also occurred. The transformation of Sb species during the manufacturing processes must also be considered because the brake pad is molded under high-temperature (200–300 °C) and high-pressure (50 MPa) conditions.

In summary, drastic changes in the chemical forms of Sb compounds are most likely to occur during both the manufacturing processes of Sb-containing products and the emission processes of Sb to the atmosphere. Subsequently, Sb in fine APM may partially transform to organometallic species during environmental circulation.

4. Conclusion

The atmospheric circulation of airborne particulate matter (APM) plays an important role in the global expansion of environmental contamination with potentially toxic Sb. Under this circumstance, there are growing concerns regarding the health risks caused by inhalation exposure to airborne Sb. Hence, more information regarding both the particle size and oxidation states of Sb in APM is required. Taking this into consideration, we believed that the selective and sensitive plasma spectroscopic application provided by HPLC-ICP-MS is essential in the fields of atmospheric sciences. The size distribution of Sb concentration exhibits a bimodal profile with peaks, one corresponding to fine (0.50–0.70 μm) and the other to coarse (3.6–5.2 μm) fractions. Sb(III) is predominant in the coarse fractions whereas Sb(V) is distributed in both the fine and coarse fractions. The presented high-resolution size distributions of Sb(III) and Sb(V) in APM suggests that the health risks by inhalation exposure to Sb and the extent of the effects of emission sources by atmospheric circulation need to be discussed. From the toxicological viewpoint, the upper part of the respiratory tracts must be focused on because of the existence of the more toxic Sb(III) compounds in coarse APM. From the environmental viewpoint, global contamination with Sb is most likely a result of the atmospheric circulation of fine APM containing Sb(V) primarily. For gaining an in-depth understanding on the biogeochemical cycles and fates of Sb, we require more information on the mechanisms of the transformation of chemical forms of Sb in its material cycle.

Acknowledgements

We are grateful for the financial supports provided by the Ministry of Education, Science, Sports and Culture, Japan, through the Grant-in-Aid for Young Scientists (B) (project number 19710022 and 19750064). A part of this research was

supported by the joint research project entitled “Characterization of nanosized particles in airborne particulate matter” at the Institute of Science and Engineering of Chuo University. We thank Ms. Misato Shimoda, Ms. Kimiyo Kumagai, Mr. Yoshinori Saitoh, Dr Hiroshi Tago, Dr Masahiro Fujita (Gunma Prefectural Institute of Public Health & Environmental Sciences), and Dr Hirokazu Kimura (National Institute of Infectious Diseases) for providing advice and technical assistance.

References

- 1 A. Iijima, K. Sato and N. Furuta, in *Airborne Particulates*, ed. M. Cheng and W. Liu, Nova Science Publishers, Inc., New York, 2009, ch. 3, pp. 81–115.
- 2 N. Furuta, A. Iijima, A. Kambe, K. Sakai and K. Sato, *J. Environ. Monit.*, 2005, **7**, 1155–1161.
- 3 D. R. Gómez, M. F. Giné, A. C. S. Bellato and P. Smichowski, *J. Environ. Monit.*, 2005, **7**, 1162–1168.
- 4 A. Iijima, H. Tago, K. Kumagai, M. Kato, K. Kozawa, K. Sato and N. Furuta, *J. Environ. Monit.*, 2008, **10**, 1025–1032.
- 5 S. Amereih, T. Meisel, R. Scholger and W. Wegscheider, *J. Environ. Monit.*, 2005, **7**, 1200–1206.
- 6 M. C. Jung, I. Thornton and H.-T. Chon, *Sci. Total Environ.*, 2002, **295**, 81–89.
- 7 W. Shotyk, M. Krachler and B. Chen, in *Biogeochemistry Availability and Transport of Metals in the Environment*, ed. A. Sigel, H. Sigel and R. K. O. Sigel, Taylor & Francis, New York, 2004, ch. 7, pp. 171–203.
- 8 J. M. Cloy, J. G. Farmer, M. C. Graham, A. B. MacKenzie and G. T. Cook, *J. Environ. Monit.*, 2005, **7**, 1137–1147.
- 9 M. Krachler, J. Zheng, R. Koerner, C. Zdanowicz, D. Fisher and W. Shotyk, *J. Environ. Monit.*, 2005, **7**, 1169–1176.
- 10 B. Venugopal and T. D. Luckey, in *Chemical Toxicity of Metals and Metalloids*, Plenum Press, New York, 1978, vol. 2, pp. 213–216.
- 11 H. R. Hansen and S. A. Pergantis, *J. Anal. At. Spectrom.*, 2008, **23**, 1328–1340.
- 12 J. Zheng, A. Iijima and N. Furuta, *J. Anal. At. Spectrom.*, 2001, **16**, 812–818.
- 13 J. Zheng, M. Ohata and N. Furuta, *Anal. Sci.*, 2000, **16**, 75–80.
- 14 M. Krachler and H. Emons, *Anal. Chim. Acta*, 2001, **429**, 125–133.
- 15 M. B. de la Calle-Guntinas, Y. Madrid and C. Camara, *Fresenius J. Anal. Chem.*, 1992, **344**, 27–29.
- 16 R. Miravet, J. F. López-Sánchez, R. Fubio, P. Smichowski and G. Polla, *Anal. Bioanal. Chem.*, 2007, **387**, 1949–1954.
- 17 T. Narukawa, A. Takatsu, K. Chiba, K. W. Riley and D. H. French, *J. Environ. Monit.*, 2005, **7**, 1342–1348.
- 18 S. Amereih, T. Meisel, E. Kahr and W. Wegscheider, *Anal. Bioanal. Chem.*, 2005, **383**, 1052–1059.
- 19 M. Filella, P. A. Williams and N. Belzile, *Environ. Chem.*, 2009, **6**, 95–105.
- 20 National Institute of Technology and Evaluation (NITE), in *Antimony and its compounds, Initial risk assessment report 19*, NITE, Tokyo, 2009, ch. 9, pp. 59–64.
- 21 D. H. Groth, L. E. Stettler, J. R. Burg, W. M. Busey, G. C. Grant and L. Wong, *J. Toxicol. Environ. Health, Part A*, 1986, **18**, 607–626.
- 22 P. E. Newton, H. F. Bolte, I. W. Daly, B. D. Pillsbury, J. B. Terrill, R. T. Drew, R. Ben-Dyke, A. W. Sheldon and L. F. Rubin, *Fundam. Appl. Toxicol.*, 1994, **22**, 561–576.
- 23 T. Gebel, *Mutat. Res., Genet. Toxicol. Environ. Mutagen.*, 1998, **412**, 213–218.
- 24 M. D. Boeck, M. Kirsch-Volders and D. Lison, *Mutat. Res., Fundam. Mol. Mech. Mutagen.*, 2003, **533**, 135–152.
- 25 R. I. McCallum, *J. Environ. Monit.*, 2005, **7**, 1245–1250.
- 26 A. Iijima, K. Sato, Y. Fujitani, E. Fujimori, Y. Saito, K. Tanabe, T. Ohara, K. Kozawa and N. Furuta, *Environ. Chem.*, 2009, **6**, 122–132.
- 27 A. Iijima, K. Sato, K. Yano, H. Tago, M. Kato, H. Kimura and N. Furuta, *Atmos. Environ.*, 2007, **41**, 4908–4919.
- 28 A. Iijima, K. Sato, K. Yano, M. Kato, K. Kozawa and N. Furuta, *Environ. Sci. Technol.*, 2008, **42**, 2937–2942.
- 29 H. R. Hansen and S. A. Pergantis, *J. Anal. At. Spectrom.*, 2006, **21**, 731–733.

-
- 30 J. Zheng, M. Ohata and N. Furuta, *Analyst*, 2000, **125**, 1025–1028.
- 31 L. M. Smith, P. J. Craig and R. O. Jenkins, *Chemosphere*, 2002, **47**, 401–407.
- 32 K. Müller, B. Daus, J. Mattusch, H.-J. Stärk and R. Wennrich, *Talanta*, 2009, **78**, 820–826.
- 33 International Commission on Radiological Protection (ICRP), in *Human Respiratory Tract Model for Radiological Protection*, ICRP Publication 66, Elsevier, Amsterdam, 1994.
- 34 K. Tsunemi and H. Wada, *J. Jpn. Inst. Met.*, 2008, **72**, 91–98.
- 35 A. J. Chandler, D. S. Kosson, T. T. Eighmy, S. E. Sawell, J. Hartlén, H. A. van der Sloot, O. Hjelmar and J. Vehlou, in *Municipal Solid Waste Incinerator Residues*, Elsevier, Amsterdam, 1997.
- 36 Y. Takahashi, K. Sakuma, T. Itai, G. Zheng and S. Mitsunobu, *Environ. Sci. Technol.*, 2008, **42**, 9045–9050.
- 37 O. von Uexküll, S. Skerfving, R. Doyle and M. Braungart, *J. Clean. Prod.*, 2005, **13**, 19–31.